

# Enhanced electrochemical properties of SnO<sub>2</sub> anode by AlPO<sub>4</sub> coating

Tae-Joon Kim<sup>a</sup>, Dongyeon Son<sup>a</sup>, Jaephil Cho<sup>b,\*</sup>, Byungwoo Park<sup>a,1,2</sup>, Hoseok Yang<sup>c</sup>

<sup>a</sup> School of Materials Science and Engineering, Research Center for Energy Conversion and Storage, Seoul National University, Seoul, South Korea

<sup>b</sup> Department of Applied Chemistry, Kumoh National Institute of Technology, 188 Shin-pyung Dong, Gumi, South Korea

<sup>c</sup> Cheil Industries, Gumi, South Korea

Received 10 June 2003; accepted 5 April 2004

Available online 15 June 2004

## Abstract

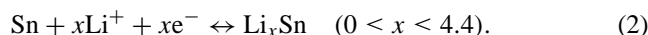
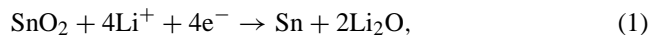
A SnO<sub>2</sub> anode material undergoes severe capacity loss, which is mainly associated with cracking/crumbling of the material by the large volume change between the Li<sub>x</sub>Sn and Sn phases, and the intensive reactions with the electrolyte solution. However, AlPO<sub>4</sub> nanoparticle coating showed drastically improved electrochemical properties with decreased surface cracks. The AlPO<sub>4</sub>-coated SnO<sub>2</sub> exhibited a capacity of 781 mAh/g, approaching its theoretical capacity at the first cycle, with 44% capacity retention after 15 cycles between 2.5 and 0 V at a relatively high C rate of 105 mA/g. In contrast, the bare SnO<sub>2</sub> showed an initial capacity of 680 mAh/g, with only 8% capacity retention after 15 cycles. © 2004 Elsevier Ltd. All rights reserved.

**Keywords:** SnO<sub>2</sub> anode; Aluminum phosphate; Nanoparticle; Coating

## 1. Introduction

Since amorphous tin-based composite oxides were first reported, exhibiting a capacity approximately twice that of carbon (372 mAh/g), researches on anodes have been focused on the tin-based materials for high-capacity Li-ion batteries [1]. Similarly, oxide compounds consisting of 3d transition-metal oxides (CoO, FeO and CuO) have also been actively studied due to their high initial capacity over 800 mAh/g [2–4]. However, these two kinds of materials have different Li reaction mechanisms, depending on the nature of the metal.

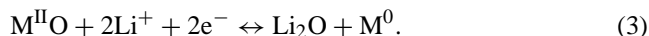
The reaction mechanisms of SnO<sub>2</sub> with lithium have been reported as [5]:



On the first discharge, the lithium bonds to the oxygen in SnO<sub>2</sub>, forming the tin metal and Li<sub>2</sub>O. Then, the Sn

alloys/dealloys up to the theoretical limit of Li<sub>4.4</sub>Sn (capacity of 783 mAh/g) [5,6]. However, SnO<sub>2</sub> has some critical problems: (i) the irreversible capacity is very large (~700 mAh/g), and the capacity fading is very severe, (ii) its cyclability depends strongly on the grain size, cutoff voltage, and charge rate [6]. For example, the capacity retention on cycling was significantly affected by the cutoff voltage: a higher cutoff voltage caused deterioration in capacity retention due to the larger volume change and destruction of the Li<sub>2</sub>O matrix holding the Sn particles [6,7]. Consequently, fracturing and a loss of contact among the grains lead to the destruction of the electrode conduction, which increases the internal resistance of the cell. The large irreversible capacity of the SnO<sub>2</sub> electrode is associated with both the bulk formation of Li<sub>2</sub>O, and intense surface reactions with the Li–Sn compounds and the electrolyte solution [5–15].

On the other hand, non-alloy metal oxides, such as 3d transition-metal oxides (CoO, FeO and CuO), can be reversibly reduced and oxidized, coupled with the formation and destruction of lithium oxide, respectively [2–4]:



At the first discharge, the reduction reaction is similar to that of SnO<sub>2</sub>, but it is reversible. These materials were observed to react reversibly with a large amount of Li, leading to sustained capacities as high as ~700 mAh/g of CoO upon

\* Corresponding author. Tel.: +82 54 467 4462; fax: +82 54 467 4477.

E-mail addresses: [jpcho@kumoh.ac.kr](mailto:jpcho@kumoh.ac.kr) (J. Cho),

[byungwoo@snu.ac.kr](mailto:byungwoo@snu.ac.kr) (B. Park).

<sup>1</sup> Co-corresponding author.

<sup>2</sup> ISE member.

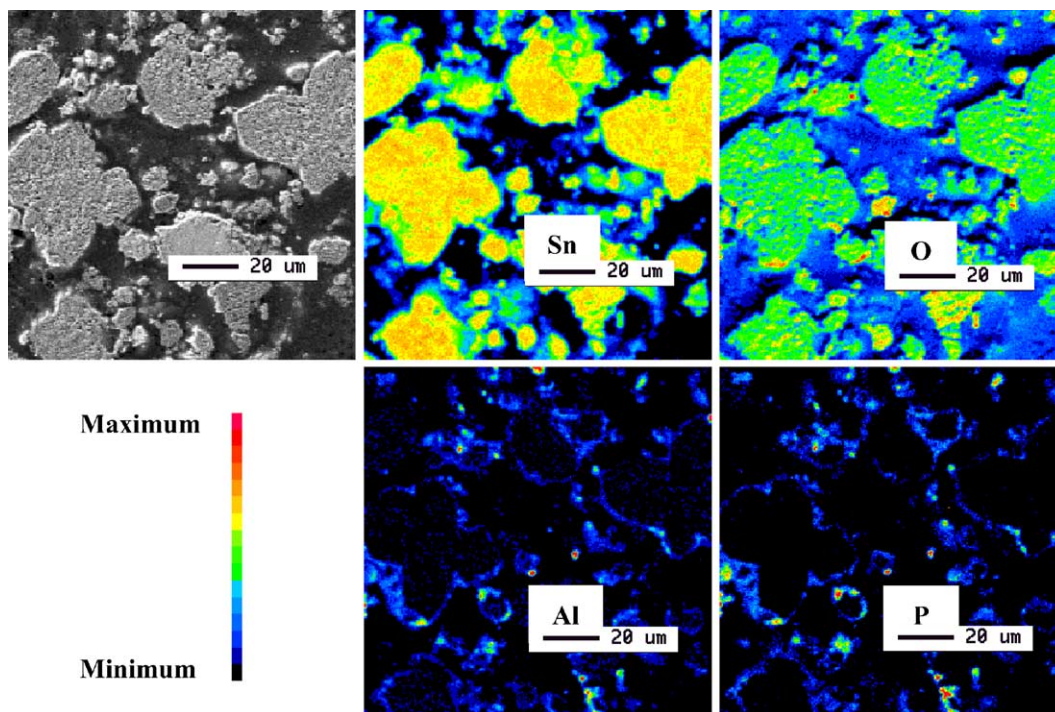


Fig. 1. EPMA mapping of  $\text{AlPO}_4$ -coated  $\text{SnO}_2$ , with Sn, O, Al, and P distributions across the cross-sectioned powders.

cycling between 3 and 0.02 V, and capacity fading is also less than that of  $\text{SnO}_2$ . However, a major limiting factor of CoO is the increased cell voltage on the subsequent cycling (showing over 1.5 V), which is approximately 0.5 V higher than  $\text{SnO}_2$ . Even though the irreversible capacity of CoO (over 320 mAh/g) is smaller than  $\text{SnO}_2$ , it still needs to be improved [3].

Recently, Cho et al. reported that a metal-oxide coating ( $\text{Al}_2\text{O}_3$ ,  $\text{ZrO}_2$ ,  $\text{TiO}_2$ , etc.) on the cathode materials can improve the cycle life and rate capability of the cathodes, and the coating layer can reduce the degradation in Li diffusivity [16–19]. In addition, a nanoparticle  $\text{AlPO}_4$  coating exhibited a much better thermal stability at higher voltages than the metal-oxide coating [20,21].

Here, the  $\text{AlPO}_4$  nanoparticle coating on  $\text{SnO}_2$  was explored for the first time to reduce the irreversible capacity and improve the cycle life of  $\text{SnO}_2$  with a potential window of 2.5–0 V at a relatively high C rate.

## 2. Experimental

$\text{SnO}_2$  was prepared from the direct oxidation of SnO in a strong acid solution with  $\text{pH} \approx 2$  for 30 min, which was followed by firing at 500 °C for 2 h. The X-ray diffraction (XRD) pattern of the powder confirmed the sole presence of tetragonal  $\text{SnO}_2$  phase.  $\text{AlPO}_4$ -coated  $\text{SnO}_2$  was prepared by the following process: Al-nitrate  $\text{Al}(\text{NO}_3)_3 \cdot 9\text{H}_2\text{O}$  (6.0 g) and  $(\text{NH}_4)_2\text{HPO}_4$  (2.2 g) were dissolved in a distilled water (30 g) until a light white-suspension solution ( $\text{AlPO}_4$  nanoparticle solution) was observed. (The pH of the coat-

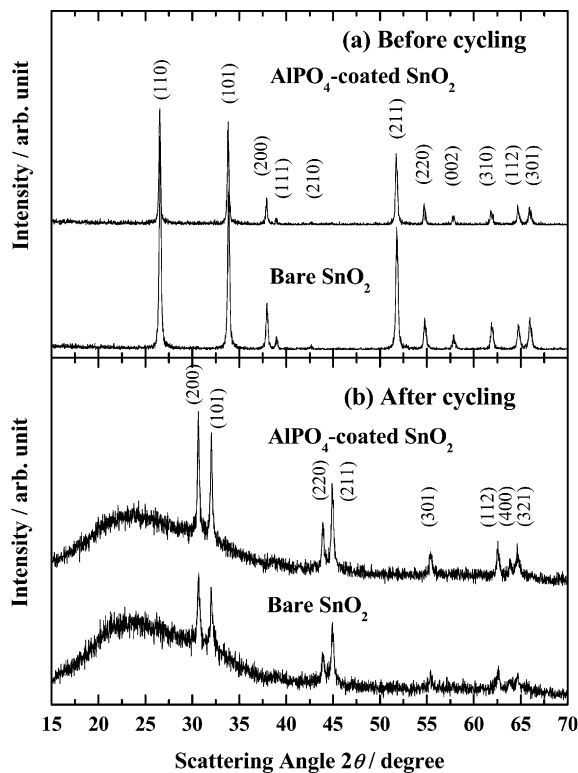


Fig. 2. XRD patterns of the bare and  $\text{AlPO}_4$ -coated  $\text{SnO}_2$ : (a) before cycling and (b) after cycling. The  $(hkl)$  diffraction indices are from tetragonal  $\text{SnO}_2$  phase in (a), and from tetragonal Sn phase in (b).

ing solution was  $\sim 2$ .) One hundred grams of SnO powder (with an average particle size of  $\sim 10 \mu\text{m}$ ) were then slowly added to the coating solution and mixed for 10 min, which was followed by drying in an oven for 6 h at  $100^\circ\text{C}$ . Subsequently, the dried powders were annealed at  $700^\circ\text{C}$  under an air-stream for 5 h in a furnace. The weight percentage by the AlPO<sub>4</sub> coating is  $\sim 1.7$  wt.% of the SnO<sub>2</sub> used.

The electrode composition was SnO<sub>2</sub>: binder: carbon black in a weight ratio of 8:1:1. The electrolyte used was 1 M LiPF<sub>6</sub> with ethylene carbonate/diethylene carbonate/ethyl-methyl carbonate (EC/DEC/EMC), and the anode was lithium metal. The cycle life of the cells was tested at a rate of  $0.045C$  ( $=35 \text{ mA/g}$ ) or  $0.134C$  ( $=105 \text{ mA/g}$ ) between a fixed voltage window of 2.5–0 V or 1.2–0 V. More binder and carbon conductor are required to overcome the disadvantage of our relatively large  $\sim 10 \mu\text{m}$  SnO<sub>2</sub> powders. Supplementary cycling experiments were performed for the better cyclability and rate capability ( $375 \text{ mA/g} = 0.48C$ ), in a weight ratio of 4:3:3 in SnO<sub>2</sub>: binder: carbon black. For the *ex situ* XRD measurements of cycled electrodes, the cells charged to 2.5 or 1.2 V after cycling were disassembled in a glove box (H<sub>2</sub>O level  $< 50$  ppm) and the SnO<sub>2</sub> powders were rinsed thoroughly with a DMC solution to remove the LiPF<sub>6</sub> salts.

### 3. Results and discussion

Fig. 1 shows electron-probe micro analysis (EPMA) mapping of the AlPO<sub>4</sub>-coated SnO<sub>2</sub> powders. To examine the distribution of Al and P elements near the particle surface, an EPMA was carried from a cross section of the AlPO<sub>4</sub>-coated SnO<sub>2</sub> powders. The result indicates that large amount of Al and P elements are observed in the vicinity of the surface, clearly confirming the AlPO<sub>4</sub> coating on the particle surface. The calculated coating thickness is  $\sim 100$  nm (with  $\sim 10 \mu\text{m}$  powder), while the measured thickness is  $\sim 1 \mu\text{m}$  (in Fig. 1), with the convolution of EPMA beam size of  $\sim 1 \mu\text{m}$ .

Fig. 2(a) shows the XRD patterns (with Cu K $\alpha$ ) of the SnO<sub>2</sub> samples before cycling. The bare and AlPO<sub>4</sub>-coated SnO<sub>2</sub> phases are tetragonal (with a space group of  $P4_2/mnm$ ), while the phase of nanoscale AlPO<sub>4</sub> coating layer does not show clear diffraction peaks. The AlPO<sub>4</sub> coating did not cause a particular change in the lattice constants,  $a$  and  $c$ , of SnO<sub>2</sub>. The bare and AlPO<sub>4</sub>-coated SnO<sub>2</sub>, respectively, exhibit  $a = (4.739 \pm 0.002) \text{ \AA}$  and  $c = (3.182 \pm 0.004) \text{ \AA}$  and  $a = (4.747 \pm 0.003) \text{ \AA}$  and  $c = (3.183 \pm 0.007) \text{ \AA}$ .

The scanning electron microscopy (SEM) images of the bare and AlPO<sub>4</sub>-coated SnO<sub>2</sub> are shown in Fig. 3(a). The bare particle consists of aggregated nano-sized grains, but

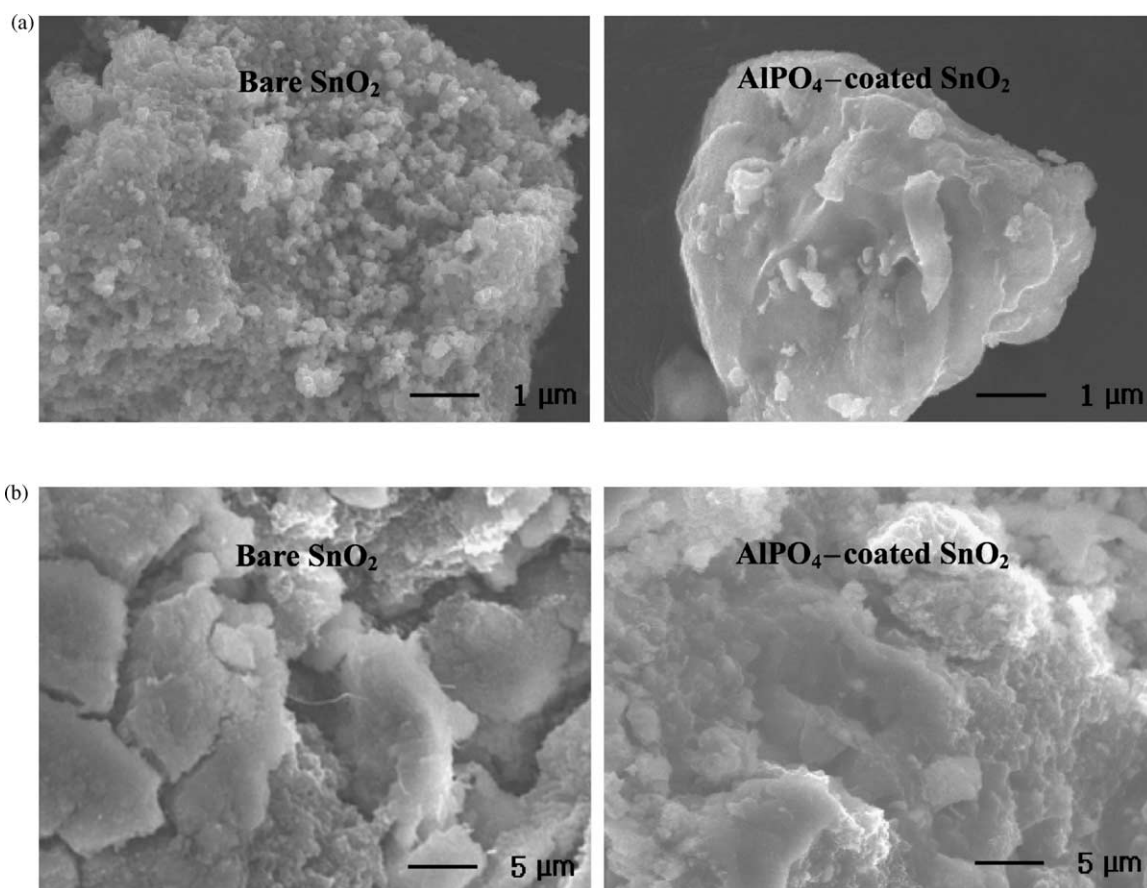


Fig. 3. SEM micrographs of the bare and AlPO<sub>4</sub>-coated SnO<sub>2</sub> particles: (a) before cycling and (b) after cycling.

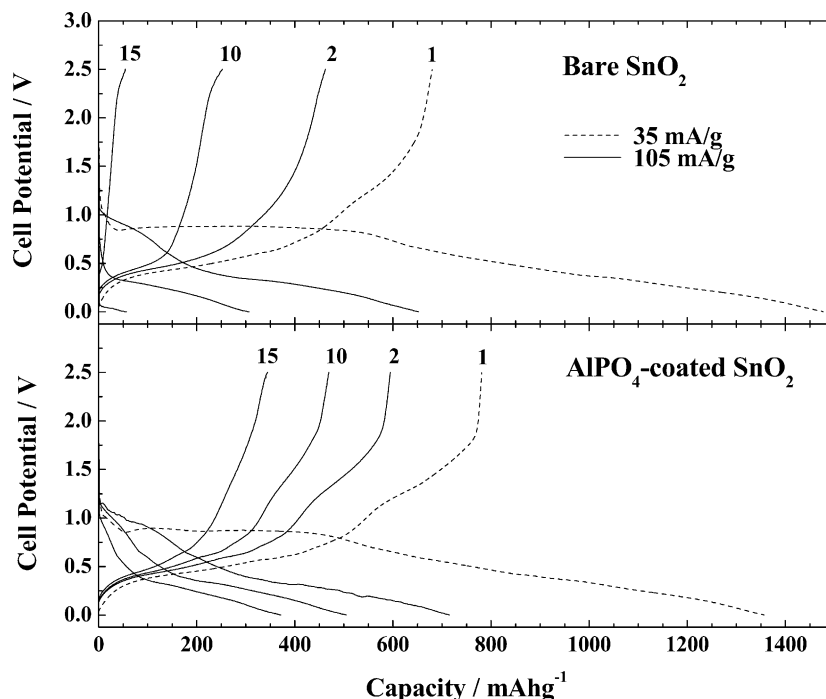


Fig. 4. Voltage profiles of the bare and  $\text{AlPO}_4$ -coated  $\text{SnO}_2$  between 2.5 and 0 V. The cells were cycled at 35 mA/g ( $=0.045C$ ) for the first discharge/charge, followed by 105 mA/g ( $=0.134C$ ) afterwards.

the  $\text{AlPO}_4$  coating led to a smooth surface morphology before cycling. Fig. 4 shows the voltage profiles of the bare and  $\text{AlPO}_4$ -coated electrodes at 35 mA/g (for the first cycle) and 105 mA/g (for subsequent cycles) between 2.5 and 0 V in the half-cells ( $\text{Li}/\text{SnO}_2$ ). The  $\text{AlPO}_4$ -coated  $\text{SnO}_2$  exhibited a capacity of 781 mAh/g, approaching its theoretical capacity at the first cycle, with 44% capacity retention (344 mAh/g) after 15 cycles. In contrast, the bare  $\text{SnO}_2$  showed an initial capacity of 680 mAh/g, with only 8% capacity retention (54 mAh/g) after 15 cycles. The  $\text{AlPO}_4$  layer is an electronic insulator, so oxidation/reduction reactions with Li ion and electron occur mainly at the interface of Sn alloy and  $\text{AlPO}_4$  coating layer, not at the interface of  $\text{AlPO}_4$  layer and electrolyte. The  $\text{AlPO}_4$  coating layer plays as a solid electrolyte, and the initial uniformly-coated layer can prevent additional formation of non-conducting passivation layer. Therefore, the  $\text{AlPO}_4$ -coated powders with decreased solid-electrolyte interface (SEI) formation showed smaller discharge capacity than the uncoated samples at the first Li-intercalation cycle, and the former exhibited larger charge capacity than the bare one at the first Li-deintercalation cycle. The reduced SEI formation may lead to higher coulombic efficiency in the coated sample.

The  $\text{AlPO}_4$ -coated  $\text{SnO}_2$  electrode cycled between 2.5 and 0 V with 105 mA/g  $C$  rate exhibited better capacity retention than the previously-reported results of Dahn's group with a nano-sized ( $\sim 5$  nm)  $\text{SnO}_2$  electrode cycled between 1.3 and 0.2 V with 37 mA/g  $C$  rate [5]. It should be noted that the nature of the lithium-insertion reaction and the stability of Li–Sn alloy phases formed depend strongly on the

particle size, potential window, and charge rate. Scrosati's group used  $\text{SnO}_2$  powders in gel-type polymer electrolyte cells. The capacity retention was good because of the plastic nature of electrolyte medium, accommodating the volume changes of the contacting electrodes. However, the initial charge capacity was low ( $\sim 450$  mAh/g) regardless of the low  $C$  rate and small particle size ( $\sim 1$   $\mu\text{m}$ ) [7]. Aurbach's group reported that nanoparticle  $\text{SnO}_2$  anode material showed relatively high charge capacity. However, these results were from the small particle size ( $\sim 5$  nm) and low charge current ( $\sim 14$  mA/g) [8].

The initial charge capacity (781 mAh/g) of the  $\text{AlPO}_4$ -coated  $\text{SnO}_2$  increased by  $\sim 100$  mAh/g compared to the bare electrode (680 mAh/g). Also, the irreversible capacity of  $\text{AlPO}_4$ -coated one is relatively small compared to the bare  $\text{SnO}_2$ . Aurbach et al. reported that the irreversible capacity in  $\text{SnO}_2$  is closely related to the intensive side reactions between the  $\text{Sn}/\text{Li}_2\text{O}$  and electrolyte species (especially  $\text{LiPF}_6$ ), generating a non-conducting passivation layer [12]. Hence, it causes a rapid increase of the impedance at the interface.

The voltage profiles of the bare and  $\text{AlPO}_4$ -coated electrodes at the rate of 105 mA/g between 1.2 and 0 V are shown in Fig. 5. The  $\text{AlPO}_4$ -coated electrode exhibited a capacity of 561 mAh/g at the first cycle, with 67% capacity retention (376 mAh/g) after 30 cycles. On the other hand, the bare electrode showed an initial capacity of 462 mAh/g, with 13% capacity retention (58 mAh/g) after 30 cycles. As expected, the limited potential window led to an improved capacity retention on cycling, compared to the voltage win-

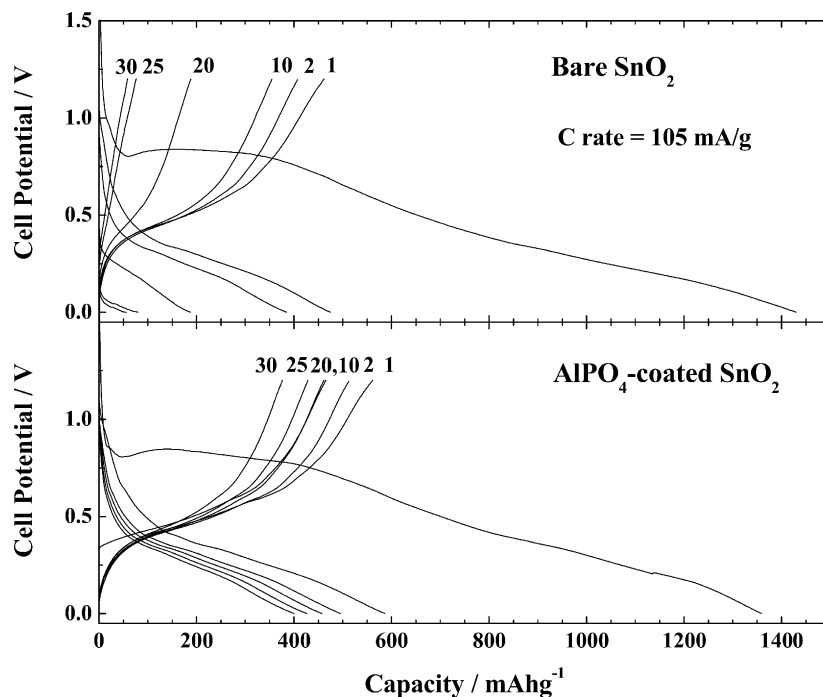


Fig. 5. Voltage profiles of the bare and AlPO<sub>4</sub>-coated SnO<sub>2</sub> at a rate of 105 mA/g (between 1.2 and 0 V).

dow of 2.5–0 V. However, the initial irreversibility of both the bare and AlPO<sub>4</sub>-coated electrodes increased compared to the 2.5–0 V window case (Fig. 4), because of the higher C rate (105 mA/g) at the first cycle. Considering that the capacity retention of SnO<sub>2</sub> anode strongly depends on the C rate, the results of Figs. 4 and 5 obtained from ~10 μm-sized

particles with AlPO<sub>4</sub> coating are clearly improved compared to the previous works from nano-sized particles [5,7,8].

Fig. 2(b) shows the XRD data of the bare and AlPO<sub>4</sub>-coated samples after 15 cycles between 2.5 and 0 V. The XRD pattern of the AlPO<sub>4</sub>-coated sample is similar to that of the bare one, showing a tetragonal Sn phase. (The broad

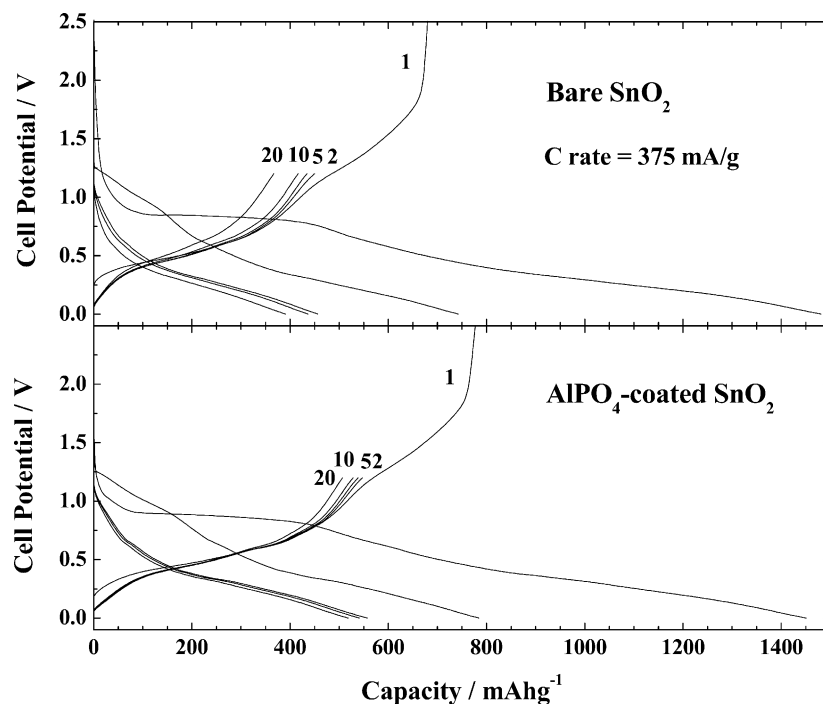


Fig. 6. Voltage profiles of the bare and AlPO<sub>4</sub>-coated SnO<sub>2</sub>, with more binder and carbon conductor, at a rate of 375 mA/g (=0.48C). The first cycle was performed between 2.5 and 0 V, followed by cycles between 1.2 and 0 V afterwards.

peak at  $\sim 25^\circ$  is associated with a glass holder.) The bare  $\text{SnO}_2$  continues to crack and crumble as a result of the large volume change on cycling, according to the reaction shown in Eq. (2). These cracking and crumbling during cycling keep generating new active surfaces that were previously passivated by the stable surface films. Hence, the repeated reaction between the electrolyte and  $\text{Sn}/\text{Li}_2\text{O}$  induces capacity fading, as shown in Fig. 4. SEM micrographs of 15-cycled bare  $\text{SnO}_2$  particles demonstrate that the grains are destroyed and covered with large cracks (Fig. 3(b)). However, such cracks are not observed in the  $\text{AlPO}_4$ -coated  $\text{SnO}_2$  particles after cycling. It is quite likely that the  $\text{AlPO}_4$  coating significantly reduces the formation of surface cracks induced from the volume change in the  $\text{Li}_x\text{Sn}$  phase, and therefore diminishes the repetitive formation of electrode/electrolyte interfaces affecting the capacity fading. More detailed experiments are currently underway to elaborate the surface microstructures of the bare and  $\text{AlPO}_4$ -coated materials after cycling.

Our electrochemical cycling tests were under severe and extreme conditions, such as larger particle size, extended voltage window, and higher  $C$  rate, compared to other reports. The improvements on the cyclability of  $\text{AlPO}_4$ -coated  $\text{SnO}_2$  are clearly observed compared to bare  $\text{SnO}_2$  anode in the extreme experimental conditions.

For the better cyclability and rate capability, the electrode composition was optimized to  $\text{SnO}_2$ : binder: carbon black in a weight ratio of 4:3:3. Additional cycling tests with these electrodes were performed at a high  $C$  rate of 375 mA/g ( $=0.48C$ ). The voltage profiles and cycle properties of the bare and  $\text{AlPO}_4$ -coated  $\text{SnO}_2$  by these electrodes are shown in Fig. 6. The  $\text{AlPO}_4$ -coated  $\text{SnO}_2$  showed the initial capacity of 778 mAh/g, close to the theoretical capacity, while the bare  $\text{SnO}_2$  had the initial capacity of 680 mAh/g for 2.5–0 V at the first cycle (similar results to Fig. 4).  $\text{AlPO}_4$  coating on the  $\text{SnO}_2$  anode led to larger initial capacity and also improved capacity retention (up to the 20th cycle) even at a high  $C$  rate, with the improved electrode composition.

In conclusion, the  $\text{AlPO}_4$ -coated  $\text{SnO}_2$  anode showed superior electrochemical properties, such as capacity fading and irreversible capacity. However, the mechanisms involved with the  $\text{AlPO}_4$  coating need to be identified. The improved electrochemical properties of the  $\text{AlPO}_4$ -coated  $\text{SnO}_2$  may be applicable to Li-ion cells.

## Acknowledgements

The authors thank Michael M. Thackeray at Argonne National Laboratory for useful discussion and Joon-Gon Lee at Seoul National University for the XRD measurements. This study was supported by Kumoh National Institute of Technology, KOSEF through the Research Center for Energy Conversion and Storage at Seoul National University, and the Center for Nanostructured Materials Technology (04K1501-01911) under the 21C Frontier Programs of the Ministry of Science and Technology.

## References

- [1] Y. Idota, T. Kubota, A. Matsufuji, Y. Maekawa, T. Miyasaka, *Science* 276 (1997) 1395.
- [2] P. Poizot, S. Laruelle, S. Grugeon, L. Dupont, J.-M. Tarascon, *Nature* 407 (2000) 496.
- [3] S. Laruelle, S. Grugeon, P. Poizot, M. Dolle, L. Dupont, J.-M. Tarascon, *J. Electrochem. Soc.* 149 (2002) A627.
- [4] P. Poizot, S. Laruelle, S. Grugeon, J.-M. Tarascon, *J. Electrochem. Soc.* 149 (2002) A1212.
- [5] I.A. Courtney, J.R. Dahn, *J. Electrochem. Soc.* 144 (1997) 2943.
- [6] I.A. Courtney, J.R. Dahn, *J. Electrochem. Soc.* 144 (1997) 2045.
- [7] S. Panero, G. Savo, B. Scrosati, *Electrochem. Solid-State Lett.* 2 (1999) 365.
- [8] J. Zhu, Z. Lu, S.T. Aruna, D. Aurbach, A. Gedanken, *Chem. Mater.* 12 (2000) 2557.
- [9] J.O. Besenhard, J. Yang, M. Winter, *J. Power Sources* 68 (1997) 87.
- [10] J. Morales, L. Sanchez, *Solid State Ionics* 126 (1999) 219.
- [11] R. Retoux, T. Brousse, D.M. Schleich, *J. Electrochem. Soc.* 146 (1999) 2472.
- [12] D. Aurbach, A. Nimberger, B. Markovsky, E. Levi, E. Sominski, A. Gedanken, *Chem. Mater.* 14 (2002) 4155.
- [13] G.R. Goward, F. Leroux, W.P. Power, G. Ouyard, W. Dmowski, T. Egami, L.F. Nazar, *Electrochem. Solid-State Lett.* 2 (1999) 367.
- [14] Y.W. Xiao, J.Y. Lee, A.S. Yu, Z.L. Liu, *J. Electrochem. Soc.* 146 (1999) 3623.
- [15] S.C. Nam, Y.H. Kim, W.I. Cho, B.W. Cho, H.S. Chun, K.S. Yun, *Electrochem. Solid-State Lett.* 2 (1999) 9.
- [16] Y.J. Kim, J. Cho, T.-J. Kim, B. Park, *J. Electrochem. Soc.* 150 (2003) A1723.
- [17] J. Cho, Y.J. Kim, T.-J. Kim, B. Park, *Chem. Mater.* 13 (2001) 18.
- [18] Y.J. Kim, T.-J. Kim, J.W. Shin, B. Park, J. Cho, *J. Electrochem. Soc.* 149 (2002) A1337.
- [19] Y.J. Kim, H. Kim, B. Kim, D. Ahn, J.-G. Lee, T.-J. Kim, D. Son, J. Cho, Y.-W. Kim, B. Park, *Chem. Mater.* 15 (2003) 1505.
- [20] J. Cho, Y.-W. Kim, B. Kim, J.-G. Lee, B. Park, *Angew. Chem. Int. Ed.* 42 (2003) 1618.
- [21] J. Cho, J.-G. Lee, B. Kim, B. Park, *Chem. Mater.* 15 (2003) 3190.